Process stress, stability and resilience in wastewater treatment processes: a novel conceptual methodology

Authors

Timothy Grant Holloway[a], John Barry Williams[a], Djamila Ouelhadj[b], Barry Cleasby[c]

University of Portsmouth, School of Civil Engineering and Surveying, Portland Building, Portland Street, Portsmouth, Hampshire, PO1 3AH

University of Portsmouth, [a]School of Civil Engineering and Surveying and [b]School of Mathematics and Physics, Portland Building, Portland Street, Portsmouth, Hampshire, PO1 3AH

[c]Southern Water Services Ltd., Durrington, Worthing, West Sussex, BN13 3NZ

E-mail address: timothy.holloway@port.ac.uk

Abstract

Stress on wastewater infrastructure and process equipment has increased dramatically due to climate change, changing consumer habits, population increase, and under investment for existing assets. These stress factors have resulted in significant fines being issued by the financial regulator Ofwat (> £6 million to UK water utilities in 2018). In addition, Ofwat's Price Review 2019 identified that UK water companies are struggling to secure the long-term resilience of their assets. In response, this research presents a simple visual methodology for characterising, both the process stress and resilience in discrete wastewater treatment processes which can be communicated simply to plant and operational management staff. Initially, the study focusses on the conceptual modelling of process stress and resilience, before moving on to how they can be de-coupled to characterise dynamic resilience. A six-step process stress evaluation methodology is presented, where; (1) is the

selection of an existing process model; (2) is data entry and includes benchmarking of existing processes; (3) is the iteration of the process model using Monte-Carlo simulations; (4) is the computation of benchmark variation; (5) is the scaling of variance, with scalar values of -1 to 0 representing process stress and 0 to 1 resilience and, (6) is the visualisation of the variance from a benchmarked condition using contour plots. The outputs of the six-step modelling process are then used to compute the probability of process failure, reliability and estimation of process stability. All the parameters are then used to identify process related failure conditions; with process stress, and resilience being visualised in a contour plot heat map. These visualisations of process stress and resilience presented here, provide a conceptual methodology that allows plant and operational managers to discretely evaluate the stress, and resilience of their wastewater treatment processes. Also, as water chemistry monitoring instrumentation for wastewater treatment processes becomes more reliable, the methodology could be adapted to provide real-time process stress visualisations for both, wastewater and chemical processes.

Keywords

Resilience, reliability, wastewater process stress analysis, benchmark, process stability, primary sedimentation

1. Introduction

In the UK, wastewater infrastructure and treatment assets are facing multiple challenges. After the privatisation of the water utilities in 1986, the evidence provided by Bayliss, (2014) suggests, that under-investment and a shrinking operational workforce has meant that many wastewater assets are not adequately maintained. Also, as identified by OWID, (2017) populations and flows are increasing, and consumer behaviour is changing with the widespread use of flushable wipes and disposable cosmetics described by CCW, (2015). This has introduced new and unique challenges for wastewater treatment plants and those that manage them. These challenges are further compounded by rising global temperatures (> 2^{o}C above pre-industrial levels) according to Hansen et al. (2010).

48 This, in turn, increases the likelihood of extreme weather events as characterised by Met office,
49 (2017). These stressors have also been identified by World economic forum, (2017), in their report on
50 global economic risk interconnections, where extreme weather events were shown to be connected
51 with water and food crises. More specifically, the hydraulic challenges (water production) are
52 particularly relevant in the UK, where ageing combined sewer systems struggle to meet demand. This
53 has left UK water utilities struggling to secure the long term resilience of their assets, and was also
54 identified in the Price Review 2019 performed by Ofwat, (2019). It has also led to increasing concern
55 over pollution events from wastewater treatment processes, which is reflected in the report provided
56 by Haymarket business media, (2018), showing that > £6 million of fines were issued to the UK water
57 utilities in 2018. As pollution incidents often relate to specific process failures, plant managers must
58 understand the level, cause and effect of process stress to inform operational management responses
59 to incidents. If suitable methods are not developed to support operational management staff in
60 understanding of existing wastewater processes, future generations will continue to be subject to
61 serious pollution incidents and the loss of the natural capital as described by Cantrell, (2019).

62 The concept of process stress could provide a simple diagnostic method for plant and
63 operational managers, allowing quick evaluation the potential process failures, while avoiding the
64 complexity of mechanistic mathematical modelling. A previous study performed by Holloway et al.
65 (2019) introduced the concept of process stress to international wastewater professionals, and 82 %
66 stated that it would be a useful tool for avoiding wastewater process-related failures. To secure the
67 long-term resilience of wastewater treatment processes, it is first crucial to understand the stresses
68 manifested within them and how this relates to accepted conventions, such as the overall resilience
69 of water supply and treatment by UK water utilities.

70 ***1.1 Mechanistic models***

71 Many studies have considered the modelling of complex physical, chemical, biochemical,
72 entropic and thermodynamic aspects of wastewater treatment systems. Research in these areas

73 extends the fundamental studies of Larsson and Skogestad, (2000), taking it from chemical
74 engineering applications, to mechanistic Plant-Wide (PWM) and Extended Plant-Wide mathematical
75 Models (E-PWM) for wastewater treatment process plants. These methods, as presented by
76 Fernández-Arévalo et al. (2014), apply PWM simulations to a wide range of complex stoichiometric
77 and thermodynamic interactions for the computation of wastewater process model outputs. The main
78 challenge in applying PWM is achieving adequate calibration as noted by Mbamba et al. (2016) and
79 Bachis et al. (2015) when considering fixed and dynamic simulations of phosphorus precipitation in
80 full-scale wastewater treatment processes. Often calibration is cumbersome and requires the analysis
81 of many wastewater parameters to ensure that the model outputs achieve a reasonable level of
82 accuracy. One extension PWM is E-PWM, which has been proposed by Fernández-Arévalo et al.
83 (2017), Juan Lema, (2017) and Solon et al. (2017). The methodology presented aims to reduce the
84 cognitive demand for process model selection by introducing a library divided into three repositories.
85 Repository (1), represents biochemical, chemical and physiochemical processes, repository (2),
86 provides a process model for computation of mass and heat transfer and, repository (3), selects
87 actuator models for estimation of direct operational costs.

88 Overall, the challenge of such complex modelling is in the development of industrially relevant
89 tools from research outputs. For example, Corominas et al. (2018) found that only 16 % of models
90 published in journal papers led to commercially available products, which is thought to relate to the
91 additional, non-standard data required, along with the knowledge to operate and calibrate models.
92 With the aim of PWM and E-PWM to accurately simulate wastewater process outputs, the model
93 complexity often means that the cause of discrete process failures are often overlooked. This lack of
94 simplified outputs from complex models is captured in the work of Newhart et al. (2019), where the
95 application of sophisticated methods made it difficult to communicate their outputs to operational
96 workers.

97 A crucial step in communicating complex outcomes to those with limited knowledge of the
98 complex mechanisms, is to generalise process outcomes as described by Langergraber et al. (2018).

It is vital that the development of a methodology has adequate modelling complexity, but also communicates the model outcomes at a plant and operational management level. This requires modelling to begin with a somewhat simplified model, in order to achieve the step-wise process as described by Guanghao et al. (2020). The research recommends that, at each stage of model development, only the necessary modelling complexity is used to avoid erroneous outputs.

1.2 Resilience, reliability and risk

The work of Butler et al. (2014) aimed to bring together reliability (*Rel*), risk and resilience. Reliability is most commonly associated with machines, or electric motor-driven systems and widely applied in chemical engineering applications as the inverse of the Probability of Failure (*pF*) as shown in Eq 1 and described by Butler et al. (2016). As observed by Sweetapple et al. (2018), risk has many descriptions, many of which relate to the context, or industry where the term is used. One example of a different interpretation of risk is in the work of Comas et al. (2008), where the risk of sludge bulking was analysed using fuzzy logic and three-dimensional surface plots. This deviates from the conventional risk assessment structure presented by Stephenson and Pollard, (2008), where likelihood multiplied by consequences, gives a pre-mitigation risk value. The more common industrial interpretation combines risk and intervention, in an attempt to reduce both the likelihood and consequences of an event. This is a well-established methodology, and is characterised by the risk matrix presented by HSE, (2019).

$$Rel = 1 - pF \tag{1}$$

$$S_R = \int_{t=0}^{t=i} S_t + \int_{t=0}^{t=i} P_s \tag{2}$$

$$\sigma^2 = \frac{\int_0^\infty t^2 \, S_m(t)dt}{\int_0^\infty S_m(t)dt} - t^{-2} \tag{3}$$

Where *Rel* is the reliability of a particular process, *pF* the probability of a system failing, S_R is the severity based on resilience theory, t is time, S_t is the imposed stressor (decoupled), is process stress P_s (integral not benchmark variance), σ^2 is the square of the variance and S_m the stressor or process stress magnitude.

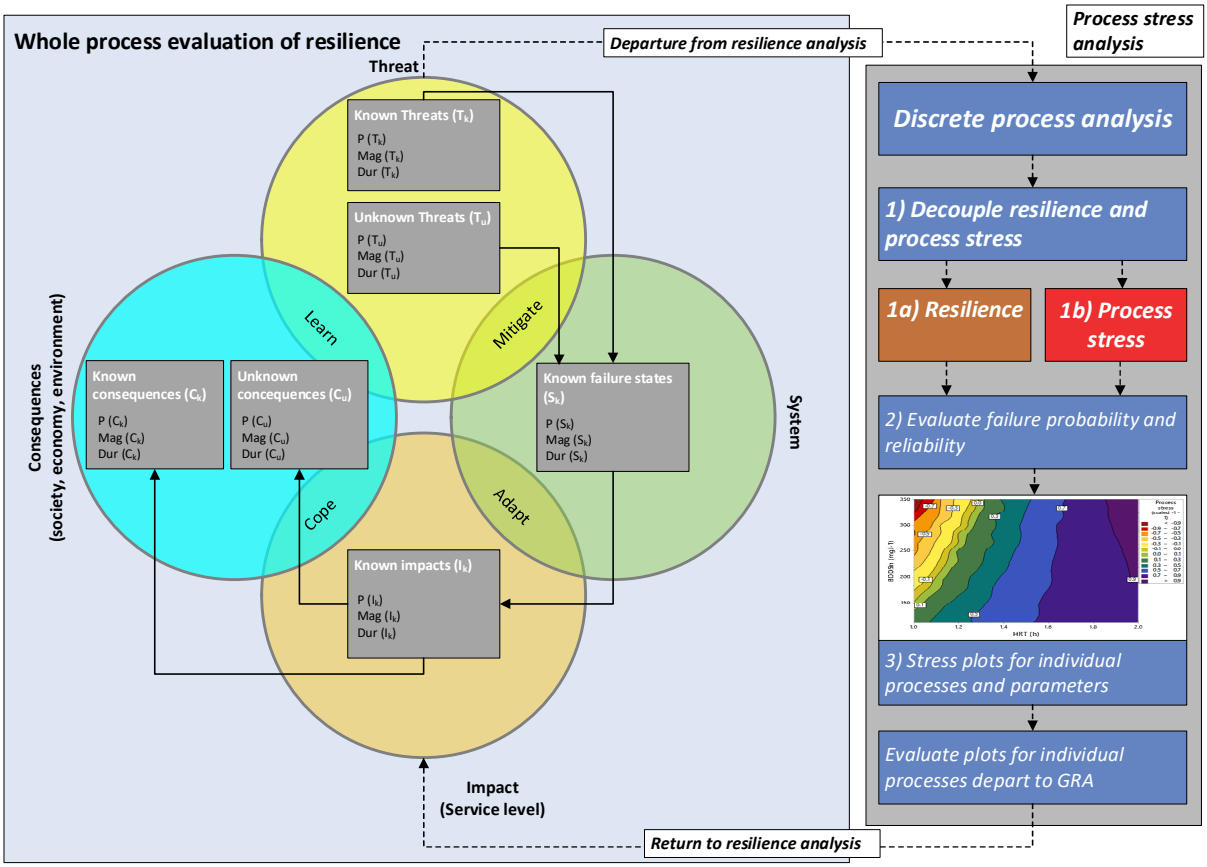

Fig. 1 *Adaption of the Safe & SuRe framework to include the analysis of wastewater treatment process stress and the recognition of dynamic resilience.*

Resilience analyses use the concept of a 'stressor' to perform a Global Resilience Analysis (GRA) which is based on the performance of a whole wastewater treatment plant. Although the stressors used in the GRA are an excellent global indicator of resilience, it can be challenging to isolate the cause and effect of an event in any one unit process (Fig. 1). In resilience theory, a stressor combines a cause-effect relationship, with the cause as the 'stressor' and the effect as 'process stress'. The characteristics of 'stressors' can be evaluated on the excess inflow or load described by Sukias et al. (2018), or toxicity from a wastewater catchment network by Napierska et al. (2018). It then follows that process stress is the negative effect of a benchmarked condition and is caused by a stressor. Some physical manifestations of process stress can be visual, such as sludge bulking or hydraulic surcharging of unit processes. However, by decoupling the stressor from process stress as shown in Fig. 1, it may be possible to depart from the conventional resilience analysis presented by Francis and Bekera, (2014) and Sweetapple et al. (2019) to evaluate the cause and the effect of an event discretely. As

shown in Fig. 2, the decoupling of the stressor from process stress means both events can be evaluated independently using a divergent, process reaction curve, geometric evaluation (Eq 3) which is similar to that described in the original work of Levenspiel, (1999). This also agrees with other studies on biochemical reactors by Holloway and Soares, (2018), where a stressor impact and the resultant process performance are mutually exclusive, dependent on chemical concentration, hydrodynamics and reactor configuration. When analysing both stressors and process stress curves independently as shown in Fig. 2, the square of variance σ^2 can be used to explain the characteristics of the reaction curves (Eq 3). Large values of σ^2 indicate an elongated curve without a highly concentrated peak, with the opposite occurring for low values according to Teefy, (1996). When considering Fig. 2, it should be noted that, although, stressors and process stresses have independent curve characteristics the sum of the integrals will be equal to the resilience-based determination of a 'severity' presented by Juan-García et al. (2017). It is anticipated that the decoupled process stress analysis will lead to an improved understanding of existing processes, especially in many cases where processes are being improved rather than replaced. The shift towards retrofitting is demonstrated in the research of Manzano, (2013) when investigating improvements to denitrifying biofilters on a wastewater treatment plant in the south of the UK.

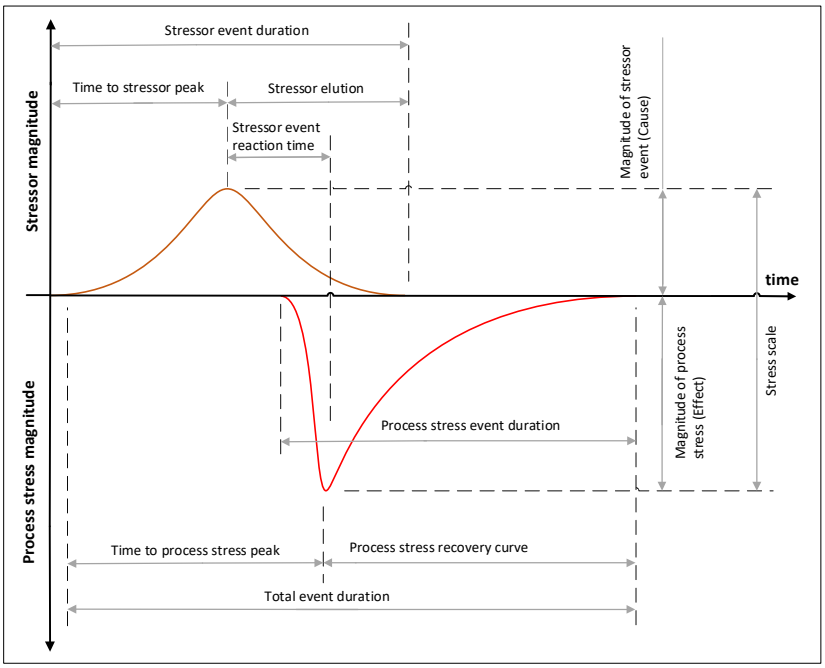

Fig. 2 *Conceptual decoupling of the stressor and process stress for wastewater treatment processes.*

To summarise, although process stress analysis is a new concept; the act of de-coupling 'stressors' from 'process stress' offers significant benefits. The first is that process stress is the missing link in understanding how discrete wastewater treatment processes react to the stressors imposed by climate change, population growth and consumer behaviour. Unlike the evaluation of a stressor in conventional GRA, process stress analysis offers the potential to understand localised stresses in discrete unit processes. Also, as on-line sensor technologies become more reliable, decoupling will give operators a reaction time to apply the correct engineering resilience interventions according to Holling, (1996), and as shown in Fig. 2. This would have significant benefits to water, wastewater, chemical and industrial process industries by identifying instantaneous process stress magnitude, and evaluating how stressor dynamics can influence the output of wastewater processes.

1.3 Resilience and dynamic resilience for wastewater treatment processes

Having identified that process stress is the negative variation from a benchmarked condition, the opposite must also be valid for a resilient process. As shown in Fig. 3, a positive variation from a benchmarked condition (green line), can also be considered resilience (surplus capacity). This indicates that process resilience occurs when wastewater processes enter a resilience event (brown line, Fig. 3), which is above what is considered a benchmark in the Benchmark Simulation Models (BSM) demonstrated by Jeppsson et al. (2007) and Copp et al. (2008).

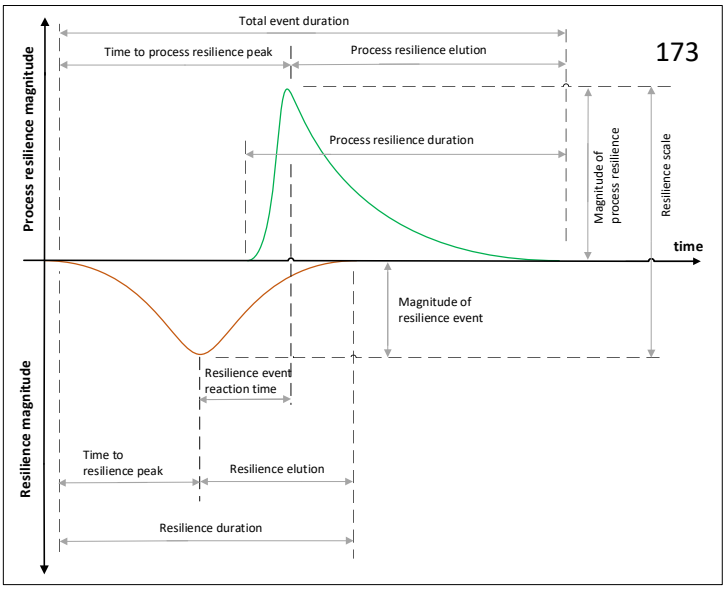

Fig. 3 Conceptual decoupling of resilience events and process resilience for wastewater treatment processes.

In a conventional wastewater treatment plant, processes can be both resilient and experience process stress. For example, an existing wastewater treatment plant with fixed dimensions will oscillate between process resilience and process stress, in response to the diurnal variations in flow and load described by Environmental protection agency, (1995) when explaining preliminary treatment methods. This means that the term 'dynamic resilience' would better encompass the diurnal variation of a process between resilience and process stress. The magnitude of variation between process resilience (Fig. 3), and process stress (Fig. 2) can be captured using Eq 4, where the ratio of the process stress to the stress scale can be used to describe the dominance of an event.

$$D_f = \frac{\delta y_e}{\delta y_{ss}} \quad (4)$$

Where D_f is the dominance factor and is the ratio of the magnitude of the event (δy_e) to the stress or resilience scale (δy_{ss}).

The conceptual evaluation of process stress presented in this paper aims to extend current resilience methodologies, to include reliability and risk, while presenting a simple methodology for visually evaluating stresses in wastewater treatment processes. A primary sedimentation tank is used to simply demonstrate the conceptual basis for evaluating stresses in wastewater treatment processes, without the vast complexity present in biological systems. To do this, a systematic evaluation is presented, incorporating existing *pF* and *Rel* parameters, but then decouples resilience and process stress to include stability. Visualisations of process stress are produced to assist plant and operational managers in identifying individual process failures, potential pollution events and anticipate changes that may occur in wastewater treatment processes.

2. Methods for systematic process stress analysis of wastewater treatment processes

The process stress analytical methodology is shown in Fig. 4 and can be explained in three stages, with each stage having an objective function. The first stage is similar to the model selection used in E-PWM, which is shown in the work of Vrecko et al. (2006) and IWA, (2018), where a process model is selected to provide the desired accuracy. The second stage is the iteration and computation of *pF* to ensure the value is representative of the modelled benchmark and inputted parameters. The

200 third stage is the computation of stress in the unit process by calculating and scaling the benchmark

201 variation between -1 and 1, where -1 is the highest level of stress and 1 the highest level of resilience.

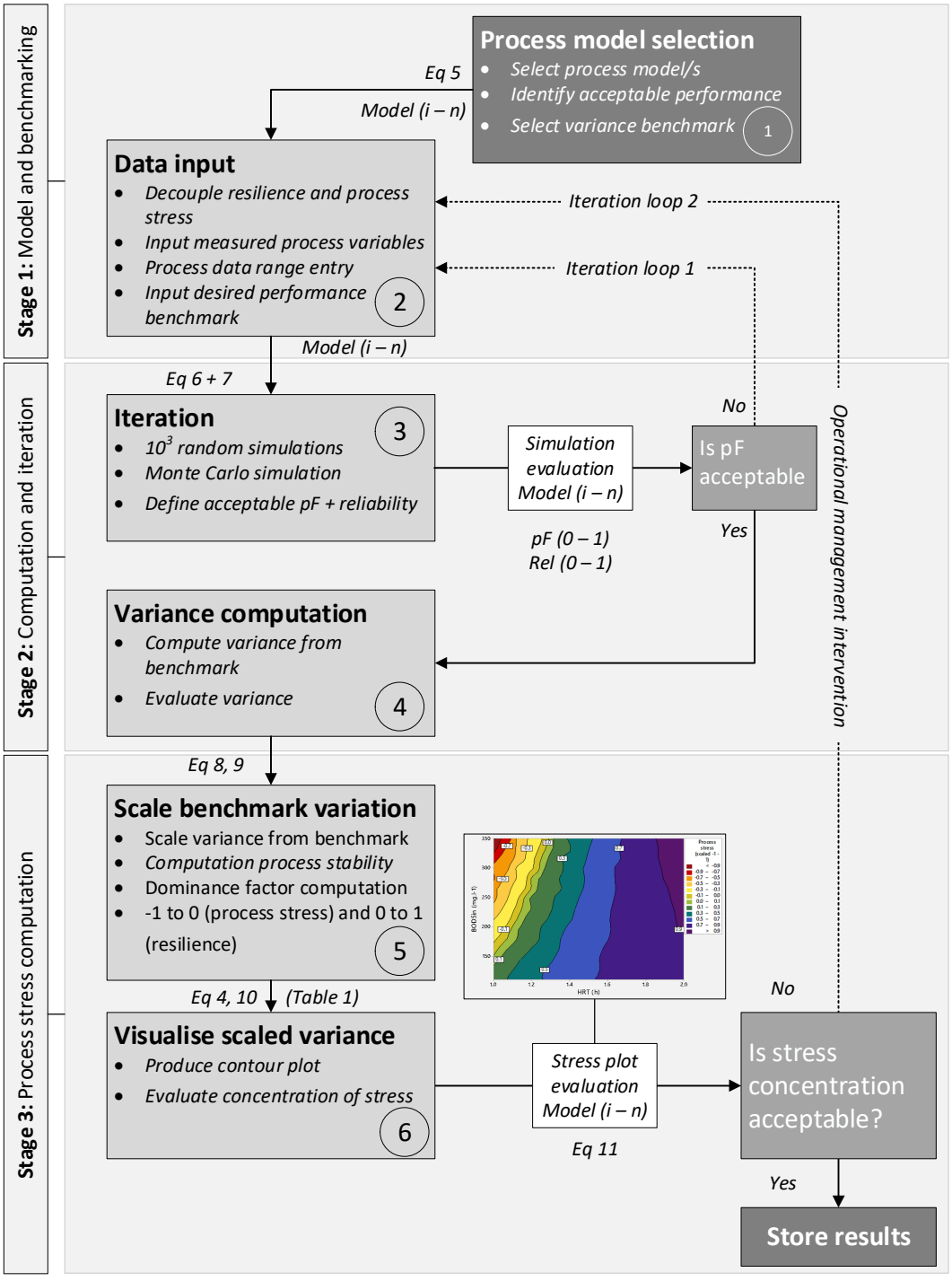

202

203 ***Fig. 4*** *Systematic analysis of process stress, with three stages and six consecutive steps, where stage 1 is the model selection*

204 *and benchmarking, stage 2 is the computation and iteration of inputted process parameters and, stage 3 is the computation*

205 *and visualisation of stresses in wastewater treatment processes.*

In addition to the three stages shown in Fig. 4, the model contains six steps, complete with two iteration loops. These steps are defined as, (1) the evaluation of the selected process model (Eq 5) and characterisation of the process benchmark condition, (2) the input of site measured process variables, ranges and desired performance targets, (3) iteration to achieve an accurate *pF*, using 10^3 pseudo-random Monte-Carlo Simulations (MCS), (4) the computation of the variance from the benchmarked conditions, (5) scaling the variation from a benchmarked conditions from -1 to 0 for stressed and 0 to 1 for resilience and (6) the production of contour plots, followed by evaluation the stress response and iteration as required.

2.1 Computation of removal efficiency in primary sedimentation (Stage 1, Fig. 4)

To investigate how a reliable conceptual model of process stress in wastewater treatment processes could be developed, a simple rectangular primary sedimentation tank model originally presented by Crites and Tchobanoglous, (1998) was selected (Eq 5). Although more complex models exist for primary sedimentation, such as those developed by Takács et al. (1991) and Otterpohl and Freund, (1992), it was decided that the simpler model would be better suited to the initial conceptual evaluation of the process stress. Mechanistic, biochemical models were not considered in this study as it was thought that the multi-variate interactions would detract from the novelty and clarity of outputs. The simple empirical model selected (Eq 5) uses Hydraulic Retention Time (*HRT*) and empirical constants to derive a removal efficiency (R_{pst}) for either BOD_5 or TSS. It also allows evaluation of, not just flow rate, but also organic and solids loading rates based on the standard concentrations published by British Water, (2013) and Tchobanoglous et al. (2013).

$$R_{pst} = \frac{t^*}{a+bt^*} \quad (5)$$

Where R_{pst} is the predicted removal efficiency, t is the HRT in h, a and b are empirical constants for BOD_5 (a = 0.018, b = 0.020) and TSS (a = 0.0075, b = 0.014). The superscript asterix highlights values used in the 10^3 pseudo-random MCS.

$$TSS_N, BOD_N = \frac{TSS^*, BOD^*}{HRT^*} \quad (6)$$

Where TSS_N, BOD_N is the normalised parameter concentration for either TSS or BOD_5, with respect to Hydraulic Retention Time (HRT) in $mg.L^{-1}.h^{-1}$. The superscript asterisk highlights values used in the 10^3 pseudo-random MCS.

2.2 Monte-Carlo simulation to compute the probability of failure (Stage 2, Fig. 4)

Originally designed to compute the probability of winning in the casinos of Monte-Carlo, the MCS method was then used in engineering applications by Siddall, (1983) and then transferred to wastewater treatment by Benedetti et al. (2011). In wastewater applications, the MCS method has been demonstrated to be robust and well suited to complex, non-linear physical, biological and chemical phenomena. Typically, an MCS is used to perform a large number of random simulations for many different scenarios both, simultaneously or consecutively. It is thought that MCS could be used to compute the probability of failure for wastewater processes, but is more commonly used for the analysis of uncertainty like that presented by Lindblom et al. (2019). MCS has not been used to evaluate the probability of failure, reliability, and stability of discrete wastewater treatment processes. As shown in Eq 7, a wastewater treatment *pF* is defined as the ability of a primary sedimentation process to meet the desired removal efficiency. Then 'IF logic', is used to provide a binary output for each of the pseudo-random simulations performed in the MCS; where 0 is assigned to X_p when a wastewater process fails ($R_t < R_d$) and 1 when a process exceeds R_d. Finally, as shown in Eq 8, *pF* is the sum of failures over the total number of random simulations. To ensure accurate outcomes from the pseudo-random simulations, *pF* was set to 10^3 after initial analyses, gave an error of < 1 %.

$$X_p = R_t - R_d \tag{7}$$

$$\begin{cases} IF\ X_p \leq 0 = 0 \\ IF\ X_p > 0 = 1 \end{cases}$$

$$pF = \frac{1 - \sum_{i=0}^{n=10^3} (X_p)}{n} \tag{8}$$

Where pF is the mean probability of failure and is based on 10^3 random simulations using R_{pst} term from Eq 1, X_p is the difference between the R_t, the theoretical removal efficiency (Eq 5) and R_d the desired removal efficiency, which take the value of one or zero. The ratio of failed results to the number of random simulations (n) is the probability of failure described by Johnson, (2017).

The Pseudo-random simulations were performed for each MCS using randomly generated values of BOD_5, TSS and HRT for the process model (Eq 5). These pseudo-random simulations were used to theoretically simulate the dynamic differences in concentration, and flow, caused by the changing characteristics of municipal wastewaters based on observations made by Atinkpahoun et al. (2018). For this study standard characterisations of wastewaters were used to demonstrate the methodology. However, for real-world applications input variables similar to that provided for compliance-based sampling under Europa, (1991) could be used.

2.3 Scaling of random simulations to compute process stress (Stage 3, Fig. 4)

To generate a scalar value to represent process stress (Eq 9), the normalised variables from Eq 6 compute the variance from a previously selected benchmarked condition (Step 4, Fig. 4). Therefore, benchmark variance is computed from the instantaneous deviation from the theoretical optimum design parameters, for a particular process shown in Eq 5. The *PS* values are then scaled to provide the Process Stress Index (*PSI*) shown in Eq 10 and 'IF logic' is used to select, either process resilience (0 to 1) or process stress (-1 to 0). These values were selected so that negative values represent process stress and positive process resilience (reserve capacity).

$$PS = Var_{Nal} - Var_{Nac} \quad (9)$$

$$PSI_{n=1} = \frac{(b-a)(PS-min)}{\max - min} + a \quad (10)$$

$$\begin{cases} IF\ PS\ \leq 0 = Scale\ [-1\ to\ 0] \\ IF\ PS\ > 0 = Scale\ [0\ to\ 1] \end{cases}$$

Where PS is process stress, to the normalised difference between allowable concentration (Var_{Nal}) and normalised actual concentration (Var_{Nac}). $PSI_{n=1}$ is the normalised, linear scaled process stress index for a single variable, b is the desired

maximum value, a is the desired minimum value, min is the minimum possible value within the random simulations for all variable ranges, max is the maximum possible value within the random simulations for all variable ranges.

$$\overline{PSI}_{i-n} = \frac{1}{n}\sum_{i=1}^{n} PSI_p \quad (11)$$

$$\overline{PSI}_{COM} = \frac{\frac{1}{n}\sum_{i=1}^{n} PSI_{BOD}+PSI_{TSS}}{2} \quad (12)$$

$$CV = \frac{S_D}{\overline{PSI}_{i-n}} \quad (13)$$

Where $\overline{PSI}_{i-n}$ is the mean PSI for all scaled outputs (10^3) from the PS evaluation (Eq 10). $\overline{PSI}_{COM}$ is the mean combined mean of the process stress indices for PSI_{BOD} and PSI_{TSS}. CV is the coefficient of variance, which normalises the standard deviation (S_D) over the $\overline{PSI}_{i-n}$.

The mean concentration of stress in a particular process ($\overline{PSI}$) was computed using each of the 10^3 simulations from Eq 11. This value was be used to display the mean stress in a particular wastewater treatment process. Table 1 shows the *PSI* descriptors and impacts of resilience and process stress on discrete wastewater processes.

Table 1 *PSI, stress level, pF and the risk to the compliance of treatment processes showing the progression of the heat map from resilient to stressed.*

Value	Descriptor	Zone	Process impact
1.00	Extreme resilience	Process resilience	**Extremely over-capacity**: extreme increase in operational costs, process capacity detriment.
0.80	Extra-large resilience		**Extra-large over-capacity**: extra-large increase in operating costs and reserve capacity
0.60	Large resilience		**Large over-capacity**: large increase in operating costs and reserve capacity
0.40	Moderate resilience		**Moderately over-capacity**: moderate increase in operating costs and reserve capacity
0.20	Mild resilience		**Mildly over-capacity**: mild increase in operating costs and reserve capacity.
0.00	Neutral	Neutral	**Correct capacity**: will vary over a diurnal profile.
-0.20	Mild process stress	Process stress	**Mildly under-capacity**: mild reduction in performance, reduction in operating costs
-0.40	Moderate process stress		**Moderately under-capacity**: moderate reduction in performance and increase in operational costs
-0.60	Large process stress		**Large under-capacity**: large reduction in performance and increase in operational costs
-0.80	Extra-large process stress		**Extra-large under-capacity**: extra-large reduction in performance and operating costs. Process failures possible.
-1.00	Extreme process stress		**Extremely under-capacity**: extreme reduction in performance, process failures and pollution incidents will occur.

Although $\overline{PSI}$ gives a good indication of process stress, it is also crucial to evaluate the variability to understand the process stability, where processes become less stable on entering stressed conditions. This was demonstrated in a study by Ødegaard and Skrøvseth, (1997) of small wastewater treatment plants in Norway, where stability was improved with the use of chemical precipitation methods. The stability of a process during the transition between resilience and stress can be evaluated from the Coefficient of Variance (*CV)* (Eq 13) and D_f (Eq 4). Two PSI_p variables can only be considered together when parameters are correlated, such as that with BOD_5 and TSS. As shown in Eq 12, a simple mean can be taken for the PSI_p for BOD_5 and TSS, resulting in $\overline{PSI}_{COM}$ (Eq 12).

To provide a simple, visual means of evaluating the stresses in wastewater treatment processes, filled contour plots were selected. Given that process stress occurs as a result of stressors from the incoming flow and load, all contour plots feature either parameter concentration or HRT on the *x-axis,* parameter concentration on *y-axis* and $\overline{PSI}_{i-n}$ or $\overline{PSI}_{COM}$ on the *z-axis*. Processes can develop stress in response to variations in flow and concentration, so a process stress heat map was plotted to display the distribution of stress based on flow and parameter concentration. This means that stresses in discrete wastewater treatment processes can be easily interpreted by plant and operational managers by tracking the colours (heat map) using the descriptors listed in Table 1.

3. Results of flow linked single-parameter process stress analysis for primary sedimentation

The initial analysis of process stress, resilience and reliability in primary sedimentation processes uses two process variables, each computes the variance from a benchmarked condition and the process stress value (dependent variable). The first variable BOD_5 has a removal efficiency (R_{pst}), which is dependent on processes retention time (*HRT*) and is influenced by diurnal flow variations (Eq 5). This dynamic variation of a wastewater treatment process, instead of the exhaustive detail of PWM, E-PWM and simulators based on ASM methodologies similar to Dudley et al. (2002), can be visualised as shown in Fig. 5 to Fig. 8. However, it should be noted that the methods presented here

can only be applied to pre-existing models, where model outputs can be scaled as the variance from a benchmarked condition.

Table 2 *Process stress model outputs.*

Input parameters						**Process stress analysis outputs**						
Nº	**Variable**	**Reference**	***HRT (h)***	***Range (y) (mg.L^{-1})***	***R_{pst}***	$\overline{PSI}$	***PSI (Median)***	***PSI (S_D)***	***PSI (CV)***	***pF***	***Rel***	D_f
1a	*HRT_{in} (x)* *BOD_{in} (y)* *PSI (z)*	Fig. 5	2 - 3	110 - 350	0.29	0.64	0.64	0.19	0.29	0.00	1.00	0.32
1b	*HRT_{in} (x)* *BOD_{in} (y)* *PSI (z)*	-	1 - 2	110 - 350	0.29	0.25	0.33	0.40	1.21	0.25	0.75	0.13
2a	*HRT_{in} (x)* *BOD_{in} (y)* *PSI (z)*	Fig. 6	1 - 2	110 - 350	0.33	-0.11	-0.14	0.34	-2.42	0.73	0.27	-0.06
2b	*HRT_{in} (x)* *BOD_{in} (y)* *PSI (z)*	-	0.5 – 1	110 - 350	0.33	-0.34	-0.29	0.19	-0.55	1.00	0.00	-0.15
3a	*HRT_{in} (x)* *TSS_{in} (y)* *PSI (z)*	Fig. 7	2 - 3	110 - 350	0.50	0.63	0.62	0.21	0.33	0.00	1.00	0.31
3b	*HRT_{in} (x)* *TSS_{in} (y)* *PSI (z)*	-	1 - 2	100 - 370	0.50	0.23	0.29	0.36	1.56	0.22	0.78	0.12
4a	*HRT_{in} (x)* *TSS_{in} (y)* *PSI (z)*	Fig. 8	1 - 2	100 - 370	0.54	-0.13	-0.12	0.33	-2.53	0.74	0.26	-0.07
4b	*HRT_{in} (x)* *TSS_{in} (y)* *PSI (z)*	-	0.5 – 1	100 - 370	0.54	-0.32	-0.27	0.19	-0.59	1.00	0.00	-0.14

Table 2 shows the process stress model inputs on the left-hand side and the model outputs on the right. The simulations in Table 2 demonstrate a moderate to large resilience (*1a*, *1b*, *3a* and *3b*) and the transition between neutral and moderate process stress (*2a*, *2b*, *4a* and *4b*) for both BOD_5 and TSS. The plotted variables from Table 2 are shown in Fig. 4 to**Fig. 7** Fig**. 8**, along with the range of values shown in the variable column.

An essential part of the process stress analysis is to evaluate *pF* and *Rel* from Table 2 in conjunction with Fig. 5 to Fig**. 8**. The *pF* gives the probability of a wastewater process failing as a result of the imposed process-related conditions (stressor), and *Rel* is how often the process is likely to fail. Both computations are largely based on the initial research of Hashimoto et al. (1982) and Kjeldsen and Rosbjerg, (2004), when investigating the reliability of water resource system operation. The Simulation in Table 2 for *1a* and *1b* (BOD_5), shows how increasing HRT can improve the resilience of a process. For example, when the HRT rises from 1 – 2 to 2 – 3 h, the *PSI* increases by 0.31, becoming more resilient. Also, *pF* reduces from 0.25 to 0.00 and the process becomes 100 % reliable. Conversely, simulation *2a* and *2b*, shows how a reduction in HRT from 1 – 2 to 0.5 – 1 h increases the mean process stress by 0.23, *pF* from 0.73 to 1.00 and reduces reliability to 0 %. The same methodology was repeated for TSS, to demonstrate high and low-stress conditions, yielding very similar outcomes. These simulation outputs match the observations made on retention tanks by Maruejouls et al. (2012), where high flows can resuspend particles causing the carry-over of carbonaceous organic matter and solids. Although operational factors such as desludging are not easily identifiable from failure and reliability analyses, the visualisation of stresses gives a robust means of identifying potential operational process failures.

Similar to the way Lizarralde *et al.* (2019) visualised the effect of TSS concentration and temperature on struvite production, contour plots were used to display the *PSI* data from the MCS. It also agrees with industrial conventions and the research of Zielinska et al. (2017) to provide a spectrum-based heat map, where red is represented by -1 (highest process stress) and blue the lowest process stress but greatest resilience at 1. The scaling of process stress is performed for the ranges shown in the 'range' column of Table 2, which cover a previously selected operating range for the primary sedimentation process. Each of the MCS was then plotted in Fig. 5 to Fig**. 8**, with HRT on the *x-axis*, BOD_5 at the inlet of the primary sedimentation vessel on the *y-axis* and *PSI* on the *z-axis*.

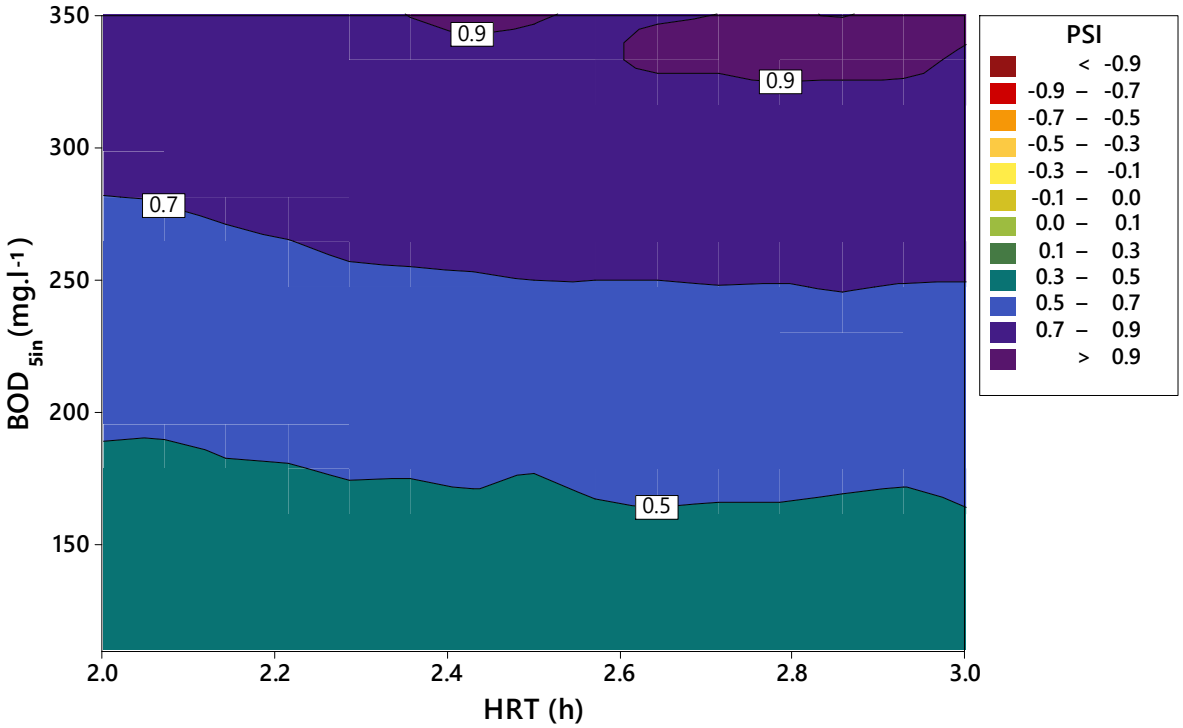

Fig. 5 *Process stress contour plot, showing HRT between 2 and 3 h, based on influent flow (x-axis). BOD_5 between 110 and 350 mg.L^{-1} (y-axis). R_{pst} used as the benchmarked condition at 0.29. PSI is shown on the z-axis, with contours showing changes in process stress (-1 to 0) or resilience (0 to 1).*

The contour plot in Fig. 5, based on simulation *1a* in Table 2 shows a moderate to extreme level of resilience (Table 1). This is evidenced in the model outputs of *PSI* at 0.64, *pF* of 0.00 and 100 % reliability. In addition, Fig. 5 shows that the primary sedimentation vessel is most resilient when the BOD_5 concentration is highest (330 – 350 mg.L^{-1}) and HRT is between 2 and 3 h. This observation agrees with Henze et al. (2008), where 60 % of the influent BOD_5 was found in the suspended (particulate). It means that as the BOD_5 concentration and HRT increases (2 – 3 h), so does particle interaction (aggregation). The opposite occurs at low BOD_5 concentrations, where the primary sedimentation process is less resilient across the HRT range (*PSI* < 0.5). In this case, particulate BOD_5, in low concentrations, experiences advection and is carried in through the vessel. This notable reduction in process performance agrees with WEF, (2005) on the engineering design of primary sedimentation processes.

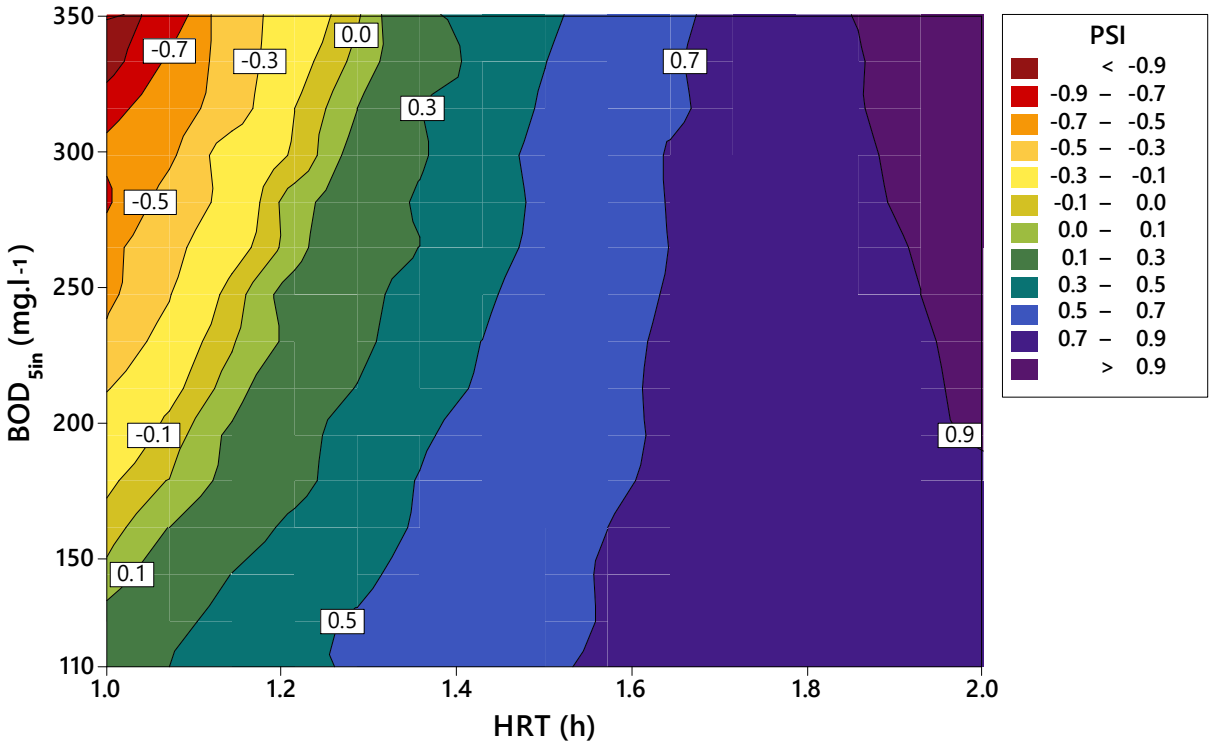

363

364 ***Fig. 6*** *Process stress contour plot, showing HRT between 1 and 2 h, based on influent flow (x-axis). BOD_5 between 110 and*
365 *350 mg.L^{-1} (y-axis). R_{pst} used as the benchmarked condition at 0.33. PSI is shown on the z-axis, with contours showing changes*
366 *in process stress (-1 to 0) or resilience (0 to 1).*

367 When the HRT is reduced (1 – 2 h), as shown in Fig. 6, the process dynamics change, displaying
368 areas of concentrated process stress. These areas of process stress, where the highest concentration
369 of *PSI* occurs (> 0.9) are seen at the highest BOD_5 concentration and the lowest HRT. This observation
370 agrees with the work on particle transport in chemical engineering processes by Coulson and
371 Richardson, (2011) and Richardson et al. (2007). They demonstrate that, a reduced HRT prevents floc
372 aggregation and gravity sedimentation from occurring, leading to the dominance of advective
373 mechanisms (Peclet number > 1). However, the mean *PSI* is -0.11 (mild process stress), and *pF* is 0.73
374 (Table 2, simulation *2a*), indicates that the primary sedimentation process will fail when the process
375 is highly loaded at a low HRT. This observation demonstrates the need for visualisation, where plant
376 and operational managers can track the possibility for process-related failures while diagnosing
377 potential threats to treatment.

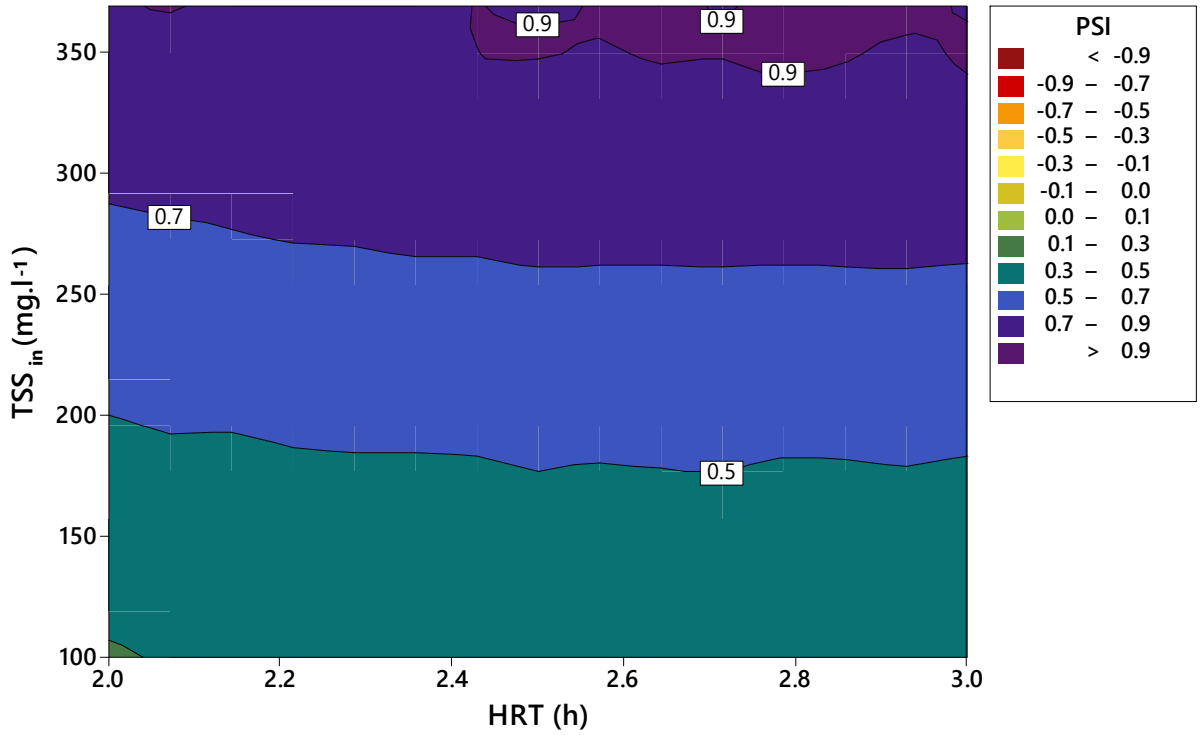

Fig. 7 *Process stress contour plot, showing HRT between 2 and 3 h, based on influent flow (x-axis). TSS between 100 and 370 mg.L^{-1} (y-axis). R_{pst} used as the benchmarked condition at 0.50. PSI is shown on the z-axis, with contours showing changes in process stress (-1 to 0) or resilience (0 to 1).*

The contour plot in Fig. 7 is based on simulation *3a* (Table 2), which, as with Fig. 5 represents a moderate to extreme level of resilience (Table 1). This is evidenced in the model outputs for *PSI* at 0.63, *pF* of 0.00 and a 100 % reliability. In a similar way to Fig. 5, lateral contour lines are present at approximately 200 mg.L^{-1} (*PSI* = 0.5) and 280 mg.L^{-1} (*PSI* = 0.7). In-addition, the highest resilience was seen between a TSS of 350 – 370 mg.L^{-1} and HRTs from 2.4 to 3 h. As with Fig. 5, this is thought to relate to mass transport mechanisms (dispersion and advection), with the addition of Stokes law, which is dependent on the size and density of particles as noted in studies of lamella clarifiers by McKean, (2010).

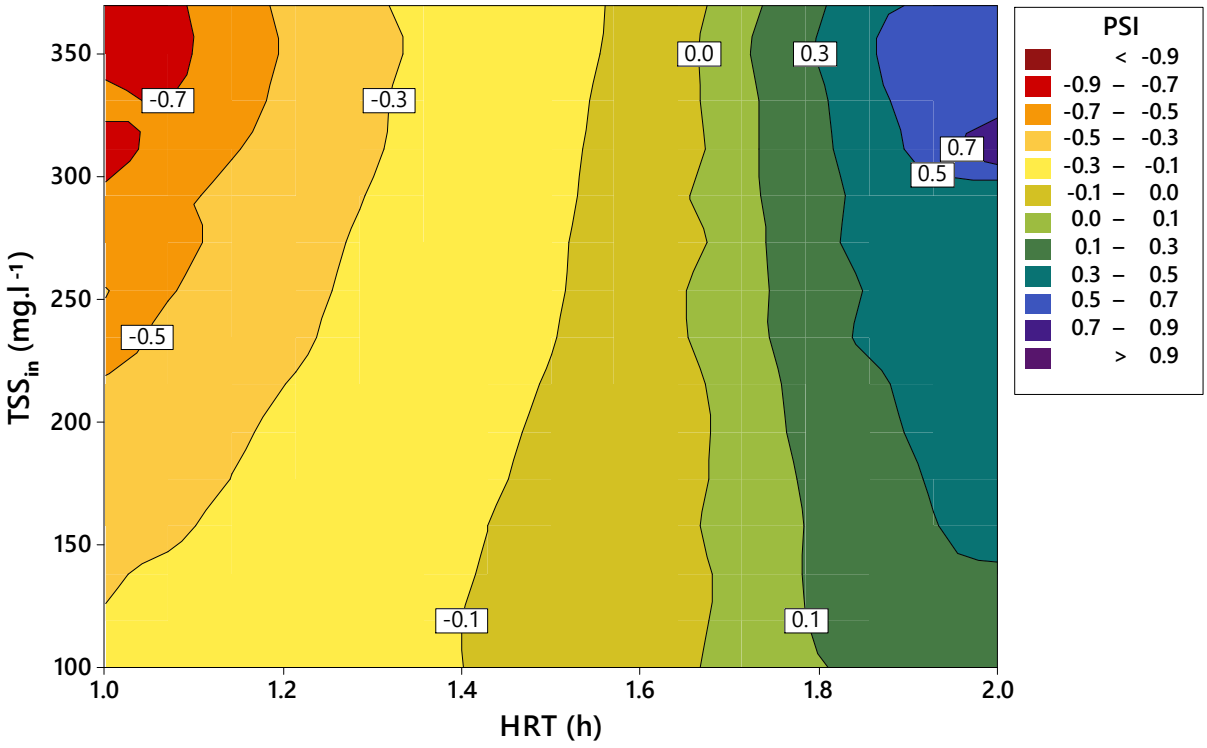

390

391 ***Fig. 8*** *Process stress contour plot, showing HRT between 1 and 2 h, based on influent flow (x-axis). TSS between 100 and 370*
392 *mg.L^{-1} (y-axis). R_{pst} used as the benchmarked condition at 0.54. PSI is shown on the z-axis, with contours showing changes in*
393 *process stress (-1 to 0) or resilience (0 to 1).*

394 When comparing Fig. 7 to Fig. 8, it is clear that reducing the HRT of a primary sedimentation
395 process increases process stress. This is demonstrated in the *PSI* of -0.13 (mild process stress), *pF* of
396 0.74 and a reliability of 26 % (Table 2, simulation *4a*). However, the primary sedimentation process
397 will fail when the process is most highly loaded at a low HRT. One interesting observation is that,
398 although sensitivity analyses do not form part of this paper, it can be seen that TSS is more sensitive
399 to changes in HRT, where process stress occupies > 50 % of Fig. 8, but < 25 % in Fig. 6. As a result, to
400 reduce computational demand, BOD_5 could be removed from the process stress analysis, using only
401 TSS. For all industries (wastewater or chemical), if correlations are possible between TSS, turbidity and
402 Chemical Oxygen Demand (COD) as noted by Azimi et al. (2019), it could enable live predictions of
403 process stress, probability of failure and reliability.

404 Overall, the contour plots and the associated Monte-Carlo methodology used to compute *pF*
405 and reliability, provides a robust approach for understanding stresses in wastewater treatment

processes. Unlike the GRA analysis presented by Mugume et al. (2015), the dynamic relationship between process stress and resilience can be simulated for individual wastewater treatment processes, while understanding the probability of a process failure and its reliability. Also, the heat map presented complies with international conventions for that analysis of risk, which allows it to be interpreted quickly by plant managers and operational staff. It is then possible for them to understand the stresses or potential failure mechanisms in individual wastewater treatment process and is not limited to a global understanding like GRA.

4. Results of load-based, two-parameter, process stress analysis for primary sedimentation

The second analysis of process stress combines BOD_5 and TSS to produce a $\overline{PSI}_{COM}$ (Eq 12), which is the mean stress of both parameters in a primary sedimentation process. The correlation between BOD_5 and TSS at 1.13 g BOD_5 for each g TSS^{-1}, noted by Puig et al. (2010), can allow the two parameters to be combined, where an increase in TSS will also increase the biologically active fraction. In other cases, the absence of inter-parameter correlations may not be possible, but here the mean stress of TSS and BOD_5 (Eq 12) can be used to explain the stresses in wastewater treatment processes. For simplification, it is acceptable to assume BOD_5 and TSS have the same HRT, as flow and load varies proportionally in municipal treatment plants as described by Butler et al. (1995).

Table 3 *Combined analysis of process stress in wastewater treatment processes when considering BOD_5 and TSS according to Eq 12, where the mean PSI is provided.*

Input parameters						**Process stress analysis outputs**						
Nº	**Variable**	**Reference**	***HRT (h)***	***Range (y) ($mg.L^{-1}$)***	R_{pst}	$\overline{PSI}_{COM}$	***PSI (Median)***	***PSI (S_D)***	***PSI (CV)***	***pF***	***Rel***	D_f
1	TSS_{in} *(x)* BOD_{in} *(y)* PSI_{ave} *(z)*	Fig. 9	2 – 3 2 – 3	100 - 370 110 - 350	0.50 0.29	0.63	0.63	0.14	0.22	0.00	1.00	0.32
2	TSS_{in} *(x)* BOD_{in} *(y)* PSI_{ave} *(z)*	Fig. 10	1 – 2 1 – 2	100 - 370 110 - 350	0.54 0.33	-0.04	-0.08	0.26	-6.50	0.69	0.31	-0.02

3	*TSS_{in} (x)* *BOD_{in} (y)* *PSI_{ave} (z)*	Fig. 10	0.5 – 1 0.5 – 1	100 - 370 110 - 350	0.54 0.33	-0.33	-0.31	0.13	-0.39	1.00	0.00	-0.17

Each of the rows in Table 3 represent simulations and shows the transition from resilience to process stress where; (1) is low stress; (2) is neutral stress and (3) is low to moderate stress for both BOD_5 and TSS. The input (left Table 3) plotted along with the axis are shown in the variable column and figure references in the reference column. The outputted *PSI* parameters are shown on the right of Table 3 under parameters such as $\overline{PSI}_{COM}$, variance parameters and D_f.

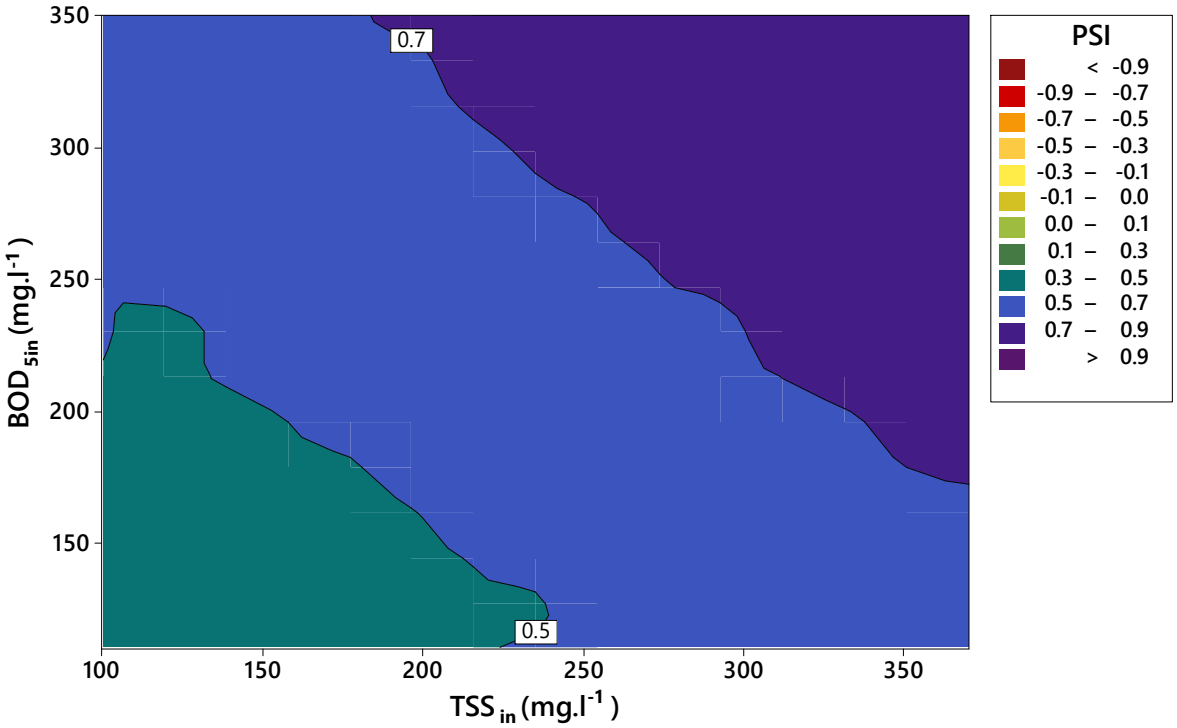

Fig. 9 *Process stress contour plot, showing HRT between 2 and 3 h, based on influent flow. TSS between 100 and 370 mg.L^{-1} (x-axis). BOD_5 between 100 and 350 mg.L^{-1} (y-axis), R_{pst} used as the benchmarked condition at 0.29 and 0.50 for BOD_5 and TSS respectively. $\overline{PSI}_{COM}$ is shown on the z-axis, with contours showing changes in process stress (-1 to 0) or resilience (0 to 1). Taken from input parameters shown in Table 3, Nº 1.*

The contour plot shown in Fig. 9 relates to simulation *1* in Table 3 and would be described as large to extra large resilience. Unlike the largely horizontal contour lines seen in Fig. 5 and Fig. 7, the contours shown in Fig. 9 are diagonal when $\overline{PSI}_{COM}$ is computed. This changes the apportionment and concentration of resilience, with the highest level of resilience triangulated between 180 - 370 and

200 - 350 mg.L^{-1} for BOD_5 and TSS. As observed in Fig. 5 and Fig**. 7**, higher concentrations increase the possibility of particle interaction and aggregation, meaning a larger proportion of the BOD_5 and TSS can be removed. The least resilience in Fig. 9 triangulates between 0 – 250 mg.L^{-1} for both BOD_5 and TSS, which again corresponds with Fig. 5 and Fig. 7 where advection dominates. Although not causing a failure, it does reduce the efficiency of the primary sedimentation process. When comparing the outputted parameters in Table 3 (simulation *1*) to Table 2 (simulation *1a* and *3a*) little difference is seen with *PSI* of 0.63, *pF* of 0.00 and a 100 % reliability.

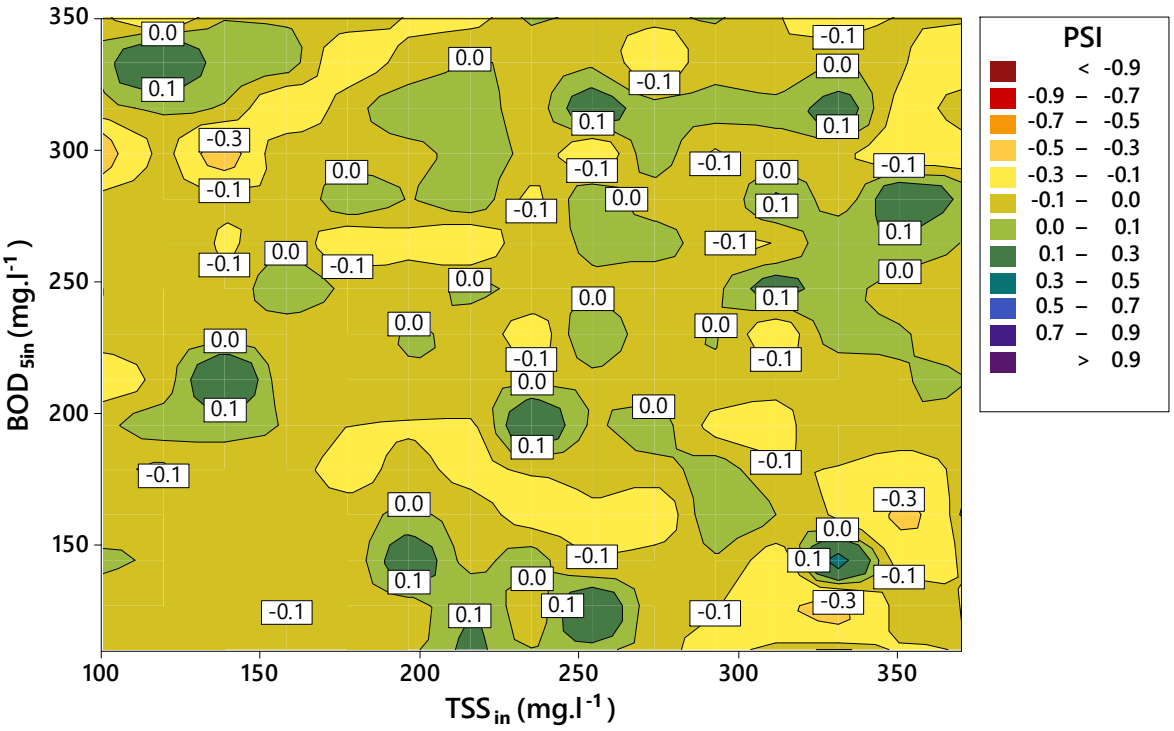

Fig. 10 *Process stress contour plot, showing HRT between 1 and 2 h, based on influent flow. TSS between 100 and 370 mg.L^{-1} (x-axis). BOD_5 between 100 and 350 mg.L^{-1} (y-axis), R_{pst} used as the benchmarked condition at 0.33 and 0.54 for BOD_5 and TSS respectively. $\overline{PSI}_{COM}$ is shown on the z-axis, with contours showing changes in process stress (-1 to 0) or resilience (0 to 1). Taken from input parameters shown in Table 3, Nº 2.*

The contour plot in Fig. 10 shows the transition from resilience to moderate process stress. Therefore, as the HRT reduces from 2 – 3 h to 1 – 2 h, stresses start to manifest, with Table 3 (simulation *2*) displaying a *PSI* of -0.04 and *pF* of 0.69. Randomised fluctuations in stresses can be seen in Fig. 10, where the *PSI* varies between 0.00 (neutral) and -0.3 (mild to moderate process stress). These randomised oscillations between neutral and moderate process stress indicate instability in the

primary sedimentation process. This means that process stability can be evaluated by analysing the magnitude and frequency of perturbations, which is evident in Table 3 (simulation *2*), where *CV* of -6.5 shows is significantly larger negative value than others in Table 3. It also indicates that a process can be stable under process stress, and when it experiences resilience. Consequently, process instability can be observed from the characteristic variation of *PSI* between stress and resilience. Presently no research has been performed to link process stress and resilience with the instability of wastewater treatment processes.

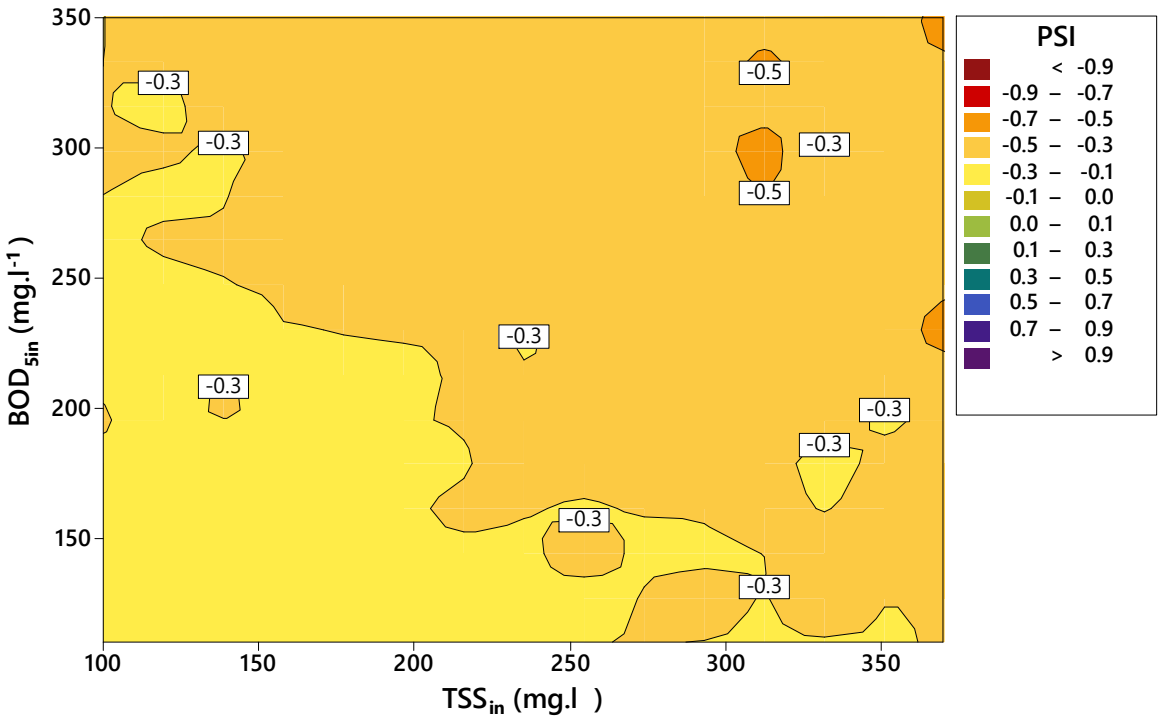

Fig. 11 *Process stress contour plot, showing HRT between 0.5 and 1 h, based on influent flow. TSS between 100 and 370 mg.L^{-1} (x-axis). BOD_5 between 100 and 350 mg.L^{-1} (y-axis), R_{pst} used as the benchmarked condition at 0.33 and 0.54 for BOD_5 and TSS respectively. $\overline{PSI}_{COM}$ is shown on the z-axis, with contours showing changes in process stress (-1 to 0) or resilience (0 to 1). Taken from input parameters shown in Table 3, Nº 3.*

The contour plot shown in Fig. 11 displays a primary sedimentation process suffering from mild to moderate stress as a result of the HRT being changed from 1 – 2 h to 0.5 – 1 h, which is evident in the *PSI* of -0.33 and *pF* of 1.00. This plot is dominated by an area (> 50 % of the plot) between -0.30 and -0.5 *PSI*, indicating light to moderate stresses are prevalent at HRT's between 0.5 and 1.0 h. The S_D and *CV* from Table 3 (simulation *3*) were evaluated to assess the stability of the process, which gave

values of 0.14 and 0.39. This indicates that, although the process is stressed, it is stable and will remain so until other parameters are changed.

Overall, the mean process stress for both BOD_5 and TSS can provide correlated process stress contour plots for wastewater treatment processes. However, some differences are observed due to the changes in contour position from BOD_5 to TSS and the mean skewing the central tendency. This means it is essential to consider the parameter correlations and inter-relationships before they are combined as they may provide unexpected or unwanted results. An interesting observation identified from the combined plots was the concept of process stability, which can also be achieved by evaluation of the variances in results using S_D and *CV* (Table 3). Stability provides a novel conceptual basis that wastewater treatment process can be stable both under resilience and also when stressed.

5. Summary of proposed methods

The potential utilisation of a methodology for the analysis of stresses in wastewater treatment processes builds on present resilience methods. To develop the conceptual basis for process stress analysis this paper; (1) defines the scale of process stress and resilience (-1 to 1); (2) proposes methods for computation of *pF, Rel* and estimation of process stability and; (3) presents the outputs visually as contour plot heat maps of wastewater process stress. These stages give operational staff the ability to observe the stresses manifested in a process, based on either, a diagnostic chart such as that shown in Fig. 5 to Fig**. 11**, or possibly automated, with a moving marker (X in Fig. 12). It indicates that plant and operational managers could visually track process stresses, and interpret changes in stressful conditions. Ultimately, these simple projections can be used to recognise how population growth and changing climatic conditions affect wastewater treatment processes.

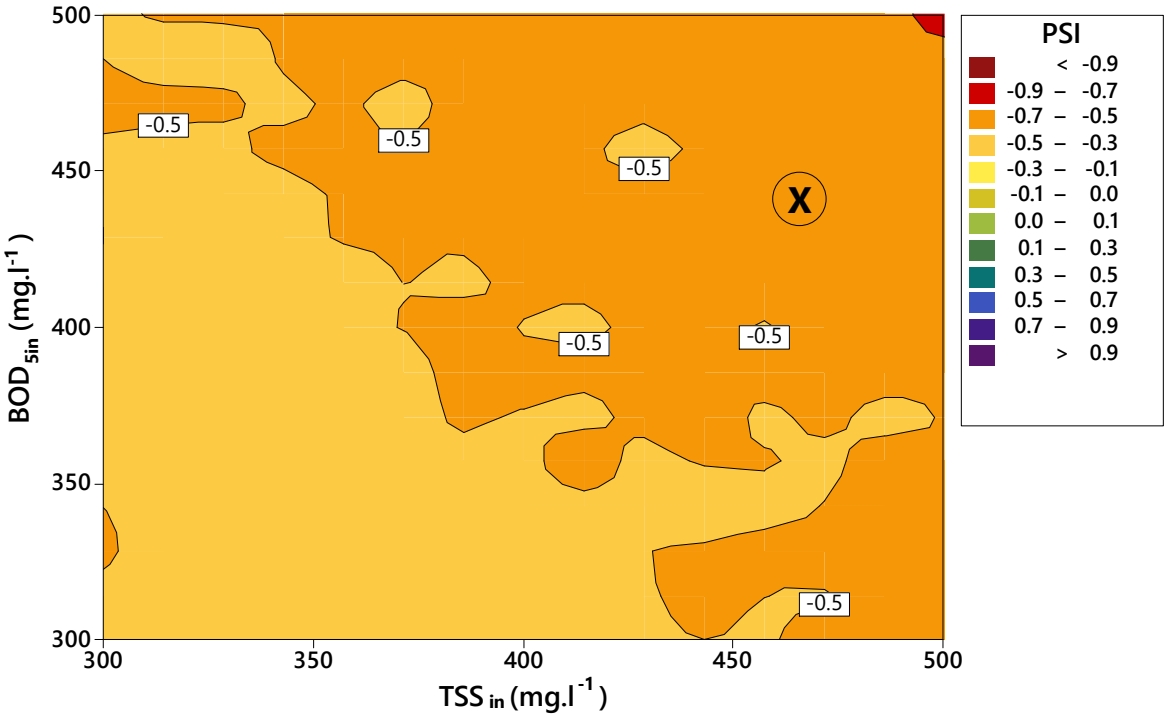

493

494 ***Fig. 12*** *Automation and control chart exploration of process stress for wastewater treatment processes, with high (300 – 500*
495 *mg.L^{-1}) for both BOD_5 and TSS, respectively. Where, HRT has been reduced to 0.1 to 0.2 h, with PSI of -0.52, pF of 1.00 and*
496 *0.00 % reliability. The (X) marker shows a theoretical operational point when the process is subject to moderate to high levels*
497 *of process stress.*

498 The process stress methodology presented in this paper provides the conceptual foundations
499 for an analytical tool that accommodates industrial norms, while reducing the computational demand
500 from that of PWM and E-PWM which require advanced knowledge to apply. In addition, the process
501 stress method explored in this paper extends existing resilience methodologies to provide an
502 improved understanding of existing wastewater treatment processes. It does this by decoupling
503 resilience (stressor) from process stress to characterise their dynamic variation over the diurnal
504 variations observed in a real wastewater treatment plant using MCS. Finally, it identifies whether a
505 process is either stressed or resilient, so operational changes avoid the potential for pollution
506 incidents, non-compliance and discrete process failures.

507

508

6. Conclusions and future perspectives

This research presents a novel conceptual methodology for the evaluation of stresses in wastewater treatment processes. It first decouples the stressor from process stress to independently evaluate their characteristics, while demonstrating the potential to visualise the impact of climate change, population growth and consumer behaviour on stresses in watewater treatment processes. A simple contour plot visualisation has been used from scaled benchmark variances and Monte-Carlo simulations to compute the probability of wastewater treatment process failures. The same contour-based visualisations were used to compute the reliability and stability of discrete unit processes. The following are the conclusions from this research:

- Process stress can be analysed by decoupling the stressor (cause) and process stress (effect). This, in turn, allows for the analysis of dynamic resilience, which is the oscillation between resilience and process stress (positive and negative benchmark variance).
- Monte-Carlo simulations can be used to perform pseudo-random simulations (within wastewater process operational ranges), from which outputs can be used to compute the probability of failure, process reliability and stability.
- Variables used in the MCS can be scaled (-1 to 1), with negative values indicating process stress and positive values resilience, which can then be plotted to produce process stress contour plots (heat map).
- Simple process stress contour plots can be easily interpreted by plant and operational managers to understand the level of stress in discrete wastewater treatment processes. This can be performed on individual parameters, or combined to understand the overall methodology of correlated parameters, such as BOD_5 and TSS.
- Process stability can also be used to evaluate the frequency and magnitude of oscillations between resilience and process stress.

The process stress methodology presented extends global resilience analyses to understand the stresses that occur in discrete wastewater treatment processes. Contour based stress plots have identified that Informed decisions can be made using a simple visual prompt to understand the negative impacts posed by climate change, population growth and changes in consumer behaviour.

The main challenge for the analysis of process stress will be applying the methodology to complex biochemical and chemical processes where many kinetic and stoichiometric parameters are used to explain wastewater process outputs. It will also be important to understand how live instrument monitoring data could be used to provide an instantaneous measure of process stress and how it could be incorporated into predictive analytics.

Role of funding sources

This research has been internally funded as a part-time PhD project by the University of Portsmouth. All materials and supervision are internally funded by the University of Portsmouth. The supervisory team are formed of two staff members from the University of Portsmouth and one from Southern Water Services Ltd.

Declaration of Competing Interest

The author has no conflicts of interest to report in the submission of this manuscript.

Acknowledgements

The University of Portsmouth funded this research, with additional support provided by Southern Water Services Ltd.

References

Atinkpahoun, C.N.H., Le, N.D., Pontvianne, S., Poirot, H., Leclerc, J.P., Pons, M.N., Soclo, H.H., 2018. Population mobility and urban wastewater dynamics. Sci. Total Environ. 622, 1431–1437. https://doi.org/10.1016/j.scitotenv.2017.12.087

556 Azimi, S.C., Shirini, F., Pendashteh, A., 2019. Evaluation of COD and turbidity removal from
557 woodchips wastewater using biologically sequenced batch reactor. Process Saf. Environ. Prot.
558 128, 211–227. https://doi.org/10.1016/j.psep.2019.05.043
559 Bachis, G., Maruéjouls, T., Tik, S., Amerlinck, Y., Melcer, H., Nopens, I., Lessard, P., Vanrolleghem, P.,
560 2015. Modelling and characterization of primary settlers in view of whole plant and resource
561 recovery modelling. Water Sci. Technol. 72, 2251–2261. https://doi.org/10.2166/wst.2015.455
562 Bayliss, K., 2014. Case study: the financialisation of Water in England and Wales. London, UK.
563 Benedetti, L., Claeys, F., Nopens, I., Vanrolleghem, P.A., 2011. Assessing the convergence of LHS
564 Monte-Carlo simulations of wastewater treatment models. Water Sci. Technol. 63, 2219–2224.
565 https://doi.org/10.2166/wst.2011.453
566 British Water, 2013. Flows and loads 4 - sizing criteria, treatment capacity for sewage treatment
567 systems. British Water, London, UK.
568 Butler, D., Farmani, R., Fu, G., Ward, S., Diao, K., Astaraie-Imani, M., 2014. A new approach to urban
569 water management: safe and sure. Procedia Eng. 89, 347–354.
570 https://doi.org/10.1016/j.proeng.2014.11.198
571 Butler, D., Friedler, E., Gatt, K., 1995. Characterising the quantity and quality of domestic wastewater
572 inflows. Water Sci. Technol. 31, 13–24. https://doi.org/10.1016/0273-1223(95)00318-H
573 Butler, D., Ward, S., Sweetapple, C., Astaraie-Imani, M., Diao, K., Farmani, R., Fu, G., 2016. Reliable,
574 resilient and sustainable water management: the safe & sure approach. Glob. Challenges 1, 63–
575 77. https://doi.org/10.1002/gch2.1010
576 Cantrell, J., The world bank, 2019. Natural capital [WWW Document]. Web Page. URL
577 https://www.worldbank.org/en/topic/natural-capital (accessed 11.30.19).
578 Comas, J., Rodríguez-Roda, I., Gernaey, K. V, Rosen, C., Jeppsson, U., Poch, M., 2008. Risk assessment
579 modelling of microbiology-related solids separation problems in activated sludge systems.
580 Environ. Model. Softw. 23, 1250–1261. https://doi.org/10.1016/j.envsoft.2008.02.013
581 Consumer council for water, 2015. Wet wipes are a growing pain in the drain for thousands of

582 blocked sewers [WWW Document]. URL https://www.ccwater.org.uk/blog/2015/11/19/wet-
583 wipes-are-a-growing-pain-in-the-drain-for-thousands-of-blocked-sewers/ (accessed 12.22.19).
584 Copp, J., Jeppsson, U., Vanrolleghem, P., 2008. The benchmark simulation models - a valuable
585 collection of modelling tools, in: 4th International Congress on Environmental Modelling and
586 Software. iEMSs, Barcelona, Spain, pp. 1314–1321.
587 Corominas, L., Garrido-Baserba, M., Villez, K., Olsson, G., Cortés, U., Poch, M., 2018. Transforming
588 data into knowledge for improved wastewater treatment operation: a critical review of
589 techniques. Environ. Model. Softw. 106, 89–103.
590 https://doi.org/10.1016/j.envsoft.2017.11.023
591 Coulson, J.M., Richardson, J.F., 2011. Chemical Engineering. Butterworth Heinemann, Oxford, UK,
592 pp. 198–212.
593 Crites, R., Tchobanoglous, G., 1998. Small and decentralized wastewater management systems, 1st
594 ed. McGraw-Hill, New York, USA.
595 Dudley, J., Buck, G., Ashley, R., Jack, A., 2002. Experience and extensions to the ASM2 family of
596 models. Water Sci. Technol. 45, 177–186.
597 Environmental protection agency, 1995. Wastewater treatment manuals - preliminary treatment, 1st
598 ed. Environmental protection agency, Wexford, Ireland.
599 Europa, 1991. Council directive. concerning urban wastewater treatment, Official Journal of the
600 European Communities. Europa, Brussels, Belgium.
601 Fernández-Arévalo, T., Lizarralde, I., Fdz-Polanco, F., Pérez-Elvira, S.I., Garrido, J.M., Puig, S., Poch,
602 M., Grau, P., Ayesa, E., 2017. Quantitative assessment of energy and resource recovery in
603 wastewater treatment plants based on plant-wide simulations. Water Res. 118, 272–288.
604 https://doi.org/10.1016/j.watres.2017.04.001
605 Fernández-Arévalo, T., Lizarralde, I., Grau, P., Ayesa, E., 2014. New systematic methodology for
606 incorporating dynamic heat transfer modelling in multi-phase biochemical reactors. Water Res.
607 60, 141–155. https://doi.org/10.1016/j.watres.2014.04.034

608 Francis, R., Bekera, B., 2014. A metric and frameworks for resilience analysis of engineered and
609 infrastructure systems. Reliab. Eng. Syst. Saf. 121, 90–103.
610 https://doi.org/10.1016/j.ress.2013.07.004
611 Guanghao, C., van Loosdrecht, M.C.M., Ekama, G., Brdjanovic, D., 2020. Biological wastewater
612 treatment: principles, modelling and design, 2nd ed. IWA publishing, London UK.
613 Hansen, J., Ruedy, R., Sato, M., Lo, K., 2010. Global surface temperature change. Rev. Geophys. 48.
614 https://doi.org/10.1029/2010RG000345
615 Hashimoto, T., Stedinger, J.R., Loucks, D.P., 1982. Reliability, resiliency and vulnarability criteria for
616 water resource system performance evaluation. Water Resour. Res. J. 18, 14–20.
617 Henze, M., van Loosdrecht, M.C.M., Ekama, G., Brdjanovic, D., 2008. Biological wastewater
618 treatment: principles, modelling and design, 1st ed. IWA publishing, London UK.
619 Holling, C.S., 1996. Engineering resilience versus ecological resilience. Eng. within Ecol. constraints.
620 Holloway, T.G., Soares, A., 2018. Influence of internal fluid velocities and media fill ratio on
621 submerged aerated filter hydrodynamics and process performance for municipal wastewater
622 treatment. Process Saf. Environ. Prot. 114, 179–191.
623 https://doi.org/10.1016/j.psep.2017.12.018
624 Holloway, T.G., Williams, J.B., Ouelhadj, D., Cleasby, B., 2019. Process stress in municipal wastewater
625 treatment processes: a new model for monitoring resilience. Process Saf. Environ. Prot. 132,
626 169–181. https://doi.org/10.1016/j.psep.2019.09.032
627 HSE, 2019. Risk based approach - risk model (initial decision matrix) [WWW Document]. URL
628 http://www.hse.gov.uk/foi/internalops/og/ogprocedures/complaints/riskmodel.pdf (accessed
629 11.25.19).
630 IWA, 2018. IWA task group on benchmarking of control strategies for WwTPs [WWW Document].
631 BSM1. URL https://iwa-network.org/groups/benchmarking-of-control-strategies-for-
632 wastewater-treatment-plants/ (accessed 12.21.19).
633 Jeppsson, U., Pons, M., Nopens, I., Alex, J., Copp, J., Gernaey, K., Rosen, C., Steyer, J., Vanrolleghem,

P., 2007. Benchmark simulation model no 2 – general protocol and exploratory case studies. Water Sci. Technol. 56, 67–78. https://doi.org/10.2166/wst.2007.604

Johnson, R., 2017. Probability and statistics for engineers, 9th ed. Pearson Education Limited, Harlow, UK.

Juan-García, P., Butler, D., Comas, J., Darch, G., Sweetapple, C., Thornton, A., Corominas, L., 2017. Resilience theory incorporated into urban wastewater systems management. State of the art. Water Res. 115, 149–161. https://doi.org/10.1016/j.watres.2017.02.047

Kjeldsen, T.R., Rosbjerg, D., 2004. Choice of reliability, resilience and vulnerability estimators for risk assessments of water resources systems. Hydrol. Sci. J. 5, 755–767.

Langergraber, G., Pressl, A., Kretschmer, F., Weissenbacher, N., 2018. Small wastewater treatment plants in Austria - technologies, management and training of operators. Ecol. Eng. 120, 164–169. https://doi.org/10.1016/j.ecoleng.2018.05.030

Larsson, T., Skogestad, S., 2000. Plantwide control - a review and new design procedure. Model. Identif. Control 21, 209–240. https://doi.org/10.4173/mic.2000.4.2

Lema, J., Suarez, S., 2017. Innovative wastewater treatment & resource recovery technologies, 1st ed. IWA publishing, London, UK. https://doi.org/10.2166/9781780407876

Levenspiel, O., 1999. Chemical reaction engineering, 3rd ed. J Wiley, Hoboken, USA.

Lindblom, E., Jeppsson, U., Sin, G., 2019. Identification of behavioral model input data sets for WWTP uncertainty analysis. Water Sci. Technol. 81, 1558–1568. https://doi.org/10.2166/wst.2019.427

Lizarralde, I., Fernández-Arévalo, T., Manas, A., Ayesa, E., Grau, P., 2019. Model-based opti mization of phosphorus management strategies in Sur WWTP, Madrid. Water Res. 153, 39–52. https://doi.org/10.1016/j.watres.2018.12.056

Manzano, I., 2013. Optimisation of denitrification in combined trickling filter and Submerged Aerated Filter (SAF) treatment plants. Cranfield University, UK.

Maruejouls, T., Vanrolleghem, P.A., Pelletier, G., Lessard, P., 2012. A phenomenological retention

660 tank model using settling velocity distributions. Water Res. 46, 6857–6867.
661 https://doi.org/10.1016/j.watres.2011.11.067
662 Mbamba, C.K., Flores-Alsina, X., Batstone, D.J., Tait, S., 2016. Validation of a plant-wide phosphorus
663 modelling approach with minerals precipitation in a full-scale WWTP. Water Res. 100, 169–183.
664 https://doi.org/10.1016/j.watres.2016.05.003
665 McKean, T., 2010. Novel application of a lamella clarifier for improved primary treatment of
666 domestic wastewater, in: 73rd Annual Water Industry Engineers and Operators' Conference.
667 WIOA, Bendigo, Australia, pp. 119–124.
668 Met office, 2017. UK extreme events - heavy rainfall and floods [WWW Document]. Web Page. URL
669 https://www.metoffice.gov.uk/research/climate/understanding-climate/uk-extreme-events-
670 _heavy-rainfall-and-floods (accessed 5.18.19).
671 Mugume, S.N., Gomez, D.E., Fu, G., Farmani, R., Butler, D., 2015. A global analysis approach for
672 investigating structural resilience in urban drainage systems. Water Res. 81, 15–26.
673 https://doi.org/10.1016/j.watres.2015.05.030
674 Napierska, D., Sanseverino, I., Loos, R., Gómez Cortés, L., Niegowska, M., Leterri, T., 2018. Modes of
675 action of the current priority pubstances list under the water framework directive and other
676 substances of interest. Luxembourg. https://doi.org/10.2760/226911
677 Newhart, K.B., Holloway, R.W., Hering, A.S., Cath, T.Y., 2019. Data-driven performance analyses of
678 wastewater treatment plants: a review. Water Res. 157, 498–513.
679 https://doi.org/10.1016/j.watres.2019.03.030
680 Ødegaard, H., Skrøvseth, A.F., 1997. An evaluation of performance and process stability of different
681 processes for small wastewater treatment plants. Water Sci. Technol. 35, 119–127.
682 https://doi.org/10.1016/S0273-1223(97)00102-9
683 Ofwat, 2019. Ofwat: PR19 Initial assessment of business plans – key documents [WWW Document].
684 Web Resour. page. URL https://www.ofwat.gov.uk/investor/pr19/ (accessed 6.18.19).
685 Otterpohl, R., Freund, M., 1992. Dynamic models for clarifiers of activated sludge plants with dry and

686 wet weather flows. Water Sci. Technol. 26, 1391–1400. https://doi.org/10.2166/wst.1992.0582
687 OWID, 2017. Future population growth [WWW Document]. Our world data. URL
688 https://ourworldindata.org/future-population-growth (accessed 3.13.19).
689 Puig, S., van Loosdrecht, M.C.M., Flameling, A.G., Colprim, J., Meijer, S.C.F., 2010. The effect of
690 primary sedimentation on full-scale WWTP nutrient removal performance. Water Res. 44,
691 3375–3384. https://doi.org/10.1016/j.watres.2010.03.024
692 Richardson, J., Harker, J., Backhurst, J., 2007. Chemical engineering: particle technology and
693 separation processes, 5th ed. Butterworth Heinemann, Burlington, USA.
694 Siddall, J., 1983. Probabilistic engineering design, 1st ed. CRC press, New York, USA.
695 Solon, K., Flores-Alsina, X., Mbamba, C.K., Ikumi, D., Volcke, E.I.P., Vaneeckhaute, C., Ekama, G.,
696 Vanrolleghem, P.A., Batstone, D.J., Gernaey, K. V, Jeppsson, U., 2017. Plant-wide modelling of
697 phosphorus transformations in wastewater treatment systems: impacts of control and
698 operational strategies. Water Res. 113, 97–110. https://doi.org/10.1016/j.watres.2017.02.007
699 Stephenson, T., Pollard, J.T., 2008. Risk management for water and wastewater utilities, 1st ed. IWA,
700 London, UK.
701 Sukias, J.P.S., Park, J.B.K., Stott, R., Tanner, C.C., 2018. Quantifying treatment system resilience to
702 shock loadings in constructed wetlands and denitrification bioreactors. Water Res. 139, 450–
703 461. https://doi.org/10.1016/j.watres.2018.04.010
704 Sweetapple, C., Astaraie-Imani, M., Butler, D., 2018. Design and operation of urban wastewater
705 systems considering reliability, risk and resilience. Water Res. 147, 1–12.
706 https://doi.org/10.1016/j.watres.2018.09.032
707 Sweetapple, C., Fu, G., Farmani, R., Butler, D., 2019. Exploring wastewater system performance
708 under future threats: does enhancing resilience increase sustainability? Water Res. 149, 448–
709 459. https://doi.org/10.1016/j.watres.2018.11.025
710 Takács, I., Patry, G.G., Nolasco, D., 1991. A dynamic model of the clarification-thickening process.
711 Water Res. 25, 1263–1271. https://doi.org/10.1016/0043-1354(91)90066-Y

712 Tchobanoglous, G., Stensel, D., Tsuchihashi, R., Burton, F., 2013. Wastewater engineering treatment
713 and resource recovery, 5th ed. Mc Graw Hill, New York, USA.
714 Teefy, S., 1996. Tracer studies in water treatment facilities: a protocol and case studies, 1st ed.
715 AWWA reaserch foundation, California, USA.
716 Vrecko, D., Gernaey, K. V, Rosen, C., Jeppsson, U., 2006. Benchmark Simulation Model No 2 in
717 Matlab-Simulink: towards plant-wide WWTP control strategy evaluation. Water Sci. Technol.
718 54, 65–72. https://doi.org/10.2166/wst.2006.773
719 WEF, 2005. Clarifier design, 2nd ed. McGraw-Hill, New York, USA.
720 World economic forum, 2017. The global risk interconnections map 2017 [WWW Document]. Web
721 page. URL http://reports.weforum.org/global-risks-2017/global-risks-landscape-2017/#risks///
722 (accessed 11.23.19).
723 Zielinska, O.A., Mayhorn, C.B., Wogalter, M.S., 2017. Connoted hazard and perceived importance of
724 fluorescent, neon, and standard safety colors. Appl. Ergon. 65, 326–334.
725 https://doi.org/10.1016/j.apergo.2017.07.011
726